Influence of Hole Diameter on Film Cooling Effectiveness over a Compound angled Gas Turbine Blade Leading Edge Surfaces

Giridhara Babu Y, Raghavan Rajendran, Anbalagan M, Felix J.
Propulsion Division,CSIR-NAL
Bangalore, Karnataka, India
giris@nal.res.in
rrajendran@nal.res.in
anbu9901000600@gmail.com
felix@nal.res.in

Ashok Babu T.P.
Mechanical Engg. Dept., NITK
Surathkal,Mangalore, Karnataka, India
tpashok@rediffmail.com

Abstract **- Gas turbine engines are highly dependent on development of blade cooling techniques for higher thermal efficiencies, among which film cooling is one of the most important technique. Investigations are conducted for the adiabatic film cooling effectiveness and heat transfer coefficients on two gas turbine blade leading edge models having the compound hole injection angles of 0, 30, 45, 55 and 60 degrees in each row along stream line direction with hole diameter of 4mm and 5.6mm respectively. Both these models are having the hole to hole pitch of 21mm. Experiments are conducted by varying the blowing ratios in the range of 1.0 to 2.50 at the density ratio of 1.30 and at a nominal flow Reynolds number of 1,00,000 based on the leading edge diameter. The blowing ratio is varied by varying the coolant mass flux with the main flow mass flux maintained at a constant rate. The density ratio of 1.30 is maintained by passing the coolant air flow through the liquid nitrogen bath at 231K and main stream air is passed at room temperature. The experimental and numerical results shows the increase in cooling effectiveness with the increase in blowing ratio upto 2.0 and found the decrease over the 2.0 for the model 1 hence, the optimized blowing ratio can be considered as 2.0 for this model. Similarly for model 2 the optimized blowing ratio is obtained as 1.50. By comparing both the models, model 2 with 5.6mm hole diameter has shown the higher film cooling effectiveness than the model 1. And heat transfer coefficient values found to be increasing with increase in blowing ratio for both these considered models.**

Keywords—film cooling; heat transfer; blowing ratio; turbine blade.

I. INTRODUCTION

Typical gas turbines are operated at higher temperatures in the range of 1000-1650 degree Celsius so the materials used for gas turbine blades should with stand high temperatures without damaging the turbine blades. The gas turbine blade leading edges are the most critical part in the turbines as they are directly hit by the exhaust gases from combustion chamber, hence the cooling of gas turbine blade leading edge surfaces is most essential.

Film cooling is used in many applications to reduce convective heat transfer to a surface. In order to increase the life of the blade and efficiency, the optimized cooling of gas turbine blade leading edge surfaces and finding the heat transfer coefficient on the blade surface is essential. Some of the examples are, film cooling of gas turbine combustion chamber liners, Rotor and stator which are subjected to high heat loads from combustion gases.

Film cooling is the introduction of a secondary fluid at one or more discrete locations along a surface exposed to a high temperature environment to protect the surface not only in the immediate region of injection but also in the downstream region as shown in Fig.1 [Gold Stein 1971].

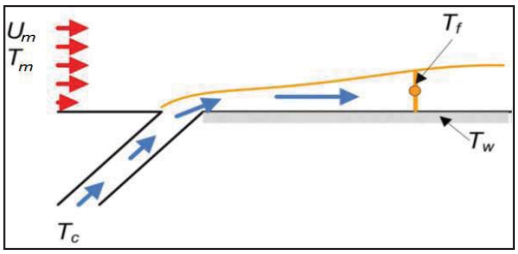

Fig. 1. Schematic of film cooling concept.

Film cooling also removes heat from the blade surface through the film hole by internal convection, $q= h_o (T_f - T_w)$, and film cooling is defined as, $\eta = (T_m - T_f) / (T_m - T_c)$. The thermal protection is expected to provide reduced heat load to

the airfoil surface. Designers need to know the net heat load into the component surface when film is injected [1].

Due to complex nature of discrete hole injection, there is need to know the local wall temperature (T_w) under the film and the gas side heat transfer coefficient with film injection. Both these components are required to estimate reduced heat load to the surface.

Film cooling primarily depends on the various geometrical and flow parameters. The major flow parameters are coolant-to hot mainstream pressure ratio (Pc/Pt), temperature ratio (Tc/Tg), and the geometrical parameters are the film cooling hole location, angle, shape, diameter, pitch and distribution of holes on a film cooled airfoil. The coolant-to-mainstream pressure ratio can be related to the coolant-to-mainstream mass flux ratio (blowing ratio) the coolant-to mainstream temperature ratio can be related to the coolant-to-mainstream density ratio. In a typical gas turbine airfoil, the blowing ratios vary approximately from 0.5 to 2.50 while the Tc/Tg values vary from 0.5 to 0.85, corresponding density ratios approximately in the range of 1.3 to 1.5 [1].

JE-Chin Han and Srinath Ekkad [2], Turbine airfoil surfaces, shrouds, blades tips and end walls are cooled by using the discrete hole film cooling. Multi row film cooling with span wise inclined film cooling holes, called showerhead, is extensively used for cooling the leading edge regions of cooled turbine vanes and blades. Film cooling protects the airfoil surface directly, compared to internal cooling technique that remove heat from the inside surface. Film cooling also removes heat from the blade surface through the film hole by internal convection. The thermal protection is expected to provide reduced heat load to the airfoil surface. Accurate and detailed local film cooling and heat transfer for turbine edge region would be useful to prevent blade failure due to local hot spots. Flow visualization, measurements and the computational predictions would provide valuable information for designing effective cooled blades for advanced gas turbines

James E. Mathew et al. [3], in their study explained about the effect of free stream turbulence on film cooling adiabatic effectiveness. It's found that high free stream turbulence is shown to increase the averaged effectiveness at high blowing rates, but decreases at low blowing rates. At low blowing rates, free stream turbulence clearly reduces the coverage area of the cooling air due to increased mixing with the main flow.

LI Shaohua Tao Peng et al. [4] in the study of numerical simulation of turbine blade film cooling with different blowing ratios and pitch using k-ϵ turbulence model showed the temperature field of different location hole rows on leading edge of turbine cascade. The cooling effectiveness of the various blowing ratios, hole to hole spacing and blade suction surface is compared and analyzed. The results show that the cooling efficiency is directly proportional to the blowing ratio and the cooling efficiency with the increasing of the blowing ratio the former decline occurs at elevated blowing ratios. Under different pitch distance conditions, the area of film cooling of the smaller pitch space is better than the bigger pitch space.

Ali Rozati et al. [5], studied the effect of coolant-mainstream blowing ratio on leading edge film cooling flow and heat transfer using Large Eddy Simulation (LES). Investigations analyzed and quantified the effects of the coolant to mainstream blowing ratio on leading edge film cooling at a Reynolds number of 100000, B.R= 0.4, 0.8 and 1.2, DR= 1 and injection angle of 30 deg.

From the above detailed literature survey, It is found the optimization of turbine blade leading edge film cooling requires the investigation of various flow and geometrical conditions like hole injection angle, hole shape, hole location, diameter of the hole, hole angle with respect to leading edge surface, hole exit to inlet area ratio (AR), coolant to mainstream blowing ratio (B.R) and density ratio (D.R). Among these parameters hole injection angle and blowing ratio has significant effect on the film cooling effectiveness, heat transfer coefficient and controlling the bleed air from the compressor.

In the present study, the two models with five rows of holes, each row having five holes with the compound angles. The holes in the adjacent rows are arranged in staggered manner. These rows of holes located one at stagnation, two rows of holes at 30 degrees either side from the stagnation and two rows of holes at 60 degrees either side from the stagnation line. The holes in each row have the compound angles of 0, 30, 45, 55 and 60 Deg. with respect to stream line direction. The test model 1 has 4mm hole diameter and model 2 has 5.6mm hole diameter with hole to hole pitch of 21mm. These models are tested to find the adiabatic film cooling effectiveness at a density ratio of 1.30 with the coolant to mainstream blowing ratios of 1.0, 1.50, 2.0 and 2.50 at a nominal flow Reynolds number of 1, 00,000 considered based on the leading edge diameter. Heat transfer coefficients are also determined experimentally at a density ratio of 1.0 and at the blowing ratio of 1.0, 1.50, 2.0 and 2.50 respectively. The experimental study was carried out over these blade leading edge models using subsonic cascade tunnel facility of CSIR-National Aerospace Laboratories, Propulsion Division, Bangalore and the respective CFD investigation was carried out using ANSYS-FLUENT solver.

II. EXPERIMENTAL SETUP AND PROCEDURE

A. Model Description

Semicircular leading edge portion of gas turbine blade is taken in our study; the test model is generated using solid works.

TABLE I. FABRICATED TURBINE BLADE LEADING EDGE MODEL DESCRIPTION

SI.No.	Model Description	Dimensions
1	Leading Edge Outer Diameter	89 mm
2	Leading Edge Inner Diameter	65 mm
3	Film Cooling Hole Diameter and Pitch for Model 1 and 2	d_1=4 mm and d_2=5.6 mm, 21mm Pitch
4	Leading Edge Model Height	210 mm
5	No. of Rows	5
6	Compound Hole Angles	0, 30, 45, 55 and 60 Deg. w.r.to Stream line direction
7	Hole Orientation Angles	0, 30 and 60 Deg along the Stagnation line

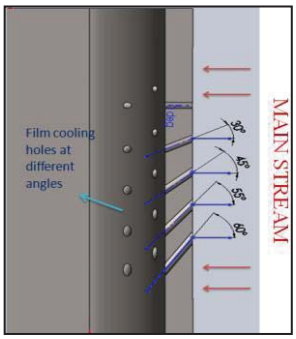

Fig. 2. Compound angled leading edge model with 0, 30, 45, 55, and 60 deg hole inclination angles w.r.to Stream line direction.

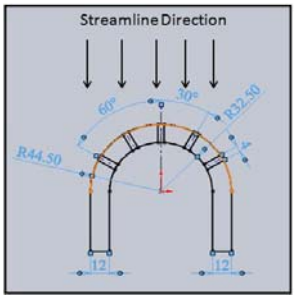

Fig. 3. Compound angled leading edge model with 0, 30 and 60 degree hole orientation angles w.r.to Stagnation line.

The geometrical details of the model are shown in Table I. The test model is fabricated using low thermal conductivity ABS-M30 material with rapid prototyping technique avoid heat losses from the gas path non-contact side to ensure adiabatic condition. The Fig. 2 shows the different hole angles used in our study and Fig. 3 shows the different hole row orientation angles with respect to stagnation line.

The test models are prepared half cylindrical with flat downstream surfaces by attaching the coolant chamber. Hard foam is filled in the model slots to have the further low thermal conductivity. The Fig. 4 and Fig. 5 shows a fabricated model of turbine blade leading edge scaled up configuration. Stainless steel sheet having thickness of 0.15mm with a required film cooling hole geometry, machined by water jet cutting is wound over the model. The S.S. sheet with an area of 260 x 160mm is connected in series by brass bus bars to supply the high current at low voltage to heat the model during heat transfer coefficient experiments. The reference thermocouples are soldered underside of the S.S sheet for applying the correction factor to the IR thermo gram data and these are routed through the model slots.

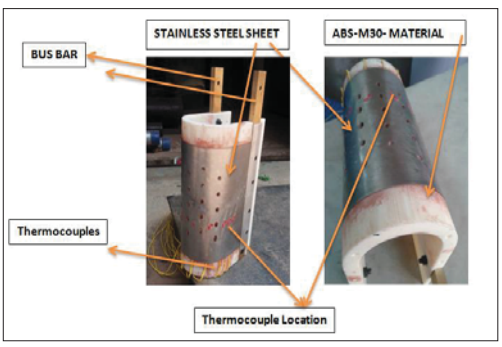

Fig. 4. Fabricated gas turbine blade Compound angled model.

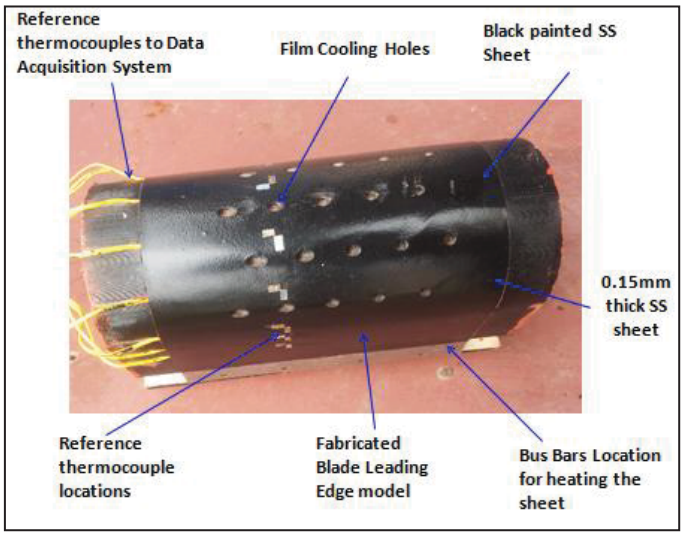

Fig. 5. Fabricated compound angled leading edge model black painted for uniform emmissivity.

B. *Experimental Setup and Procedure*

Gas turbine leading edge model is mounted in the test section, consisting of rectangular duct with a size of 320mm x 230mm x 700 mm. Experimental test facility consists of compressed air unit, settling chamber, air filter, control valve, orifice meter and rectangular duct test sections where gas turbine leading edge models are placed. Air is selected as working fluid for both mainstream and coolant. Main stream flows through the settling chamber to the test section to have the uniform flow. The main flow is controlled by the gate valve placed much ahead of settling chamber. The coolant air to the model is passed through the heat exchanger, where the controlled liquid nitrogen is used to cool the coolant air to have the required coolant temperature. The static and total pressures of mainstream flow to the inlet of test section are measured and maintained to have the required Reynolds number. The coolant flow passing through the orifice meter is also maintained by monitoring the upstream and differential pressures across the orifice meter. The required coolant flow is maintained to have the blowing ratios of 1.0, 1.50, 2.0 and 2.50. The mainstream and coolant temperatures are monitored and maintained to have the required density ratio. To measure the pressure and temperature of main stream and coolant air, pressure ports and thermocouples are incorporated at inlet and outlet of rectangular duct and at inlet to the coolant chamber as shown in Fig. 6.

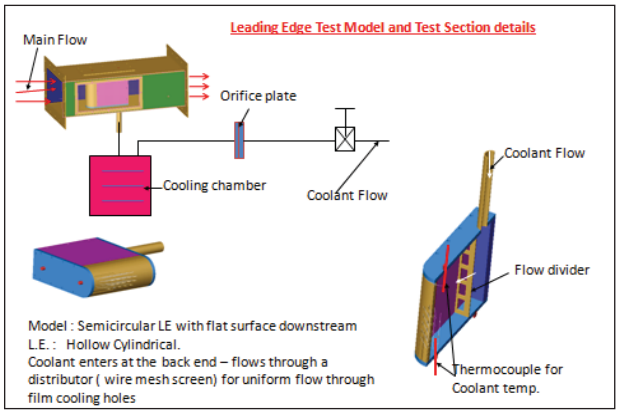

Fig. 6. Schematic of Experimental Test Setup.

The Fig. 6 shows the schematic of the experimental setup. The calibrated reference thermocouples are placed on the test model as shown in Fig. 5 at known locations, to correct thermo gram test surface data obtained by the Infra-red camera. Pressure net scanner is used for measuring pressures from pressure ports and the Fluke data acquisition is used to measure the temperatures of thermocouples during these experiments.

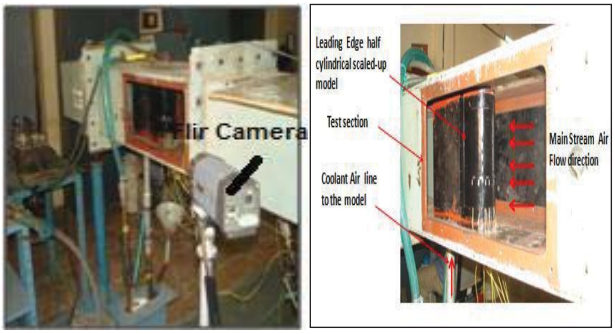

Fig. 7. Test model mounted in test section with Infra red Camera.

The air is drawn from the centralized air compressor facility of NAL, with the continuous pressure of 60psi. The gate valve is used to maintain experimental pressure at the inlet to the test rig. The rectangular test section is fully tightened to withstand with high pressure. The test section is made with the opening to view the model by infrared camera through transparent sheet as shown in Fig. 7. The provision is made to supply the coolant air to the test model through the coolant chamber. Flir make Infra-red camera is used for the non-contact type temperature measurement of the test surface as shown in Fig. 7.

C. Film Cooling Effectiveness Measurements

The main stream air is allowed to flow over the test surface and the coolant flow is passed through the coolant chamber, which ejects through the film cooling holes. The required coolant flow is maintained to have the blowing ratios i.e. the coolant to main stream mass flux ratio of 1.0, 1.50, 2.0 and 2.50. The coolant air temperature is maintained at 231K by passing the air through the liquid nitrogen heat exchanger bath to have the required density ratio i.e. the coolant to main stream density ratio of 1.30. The level of the liquid nitrogen in the bath is controlled to have the required coolant air temperature. The main stream air at ambient temperature coming from the centralized compressor facility is maintained at 24mm of H_2O to have the Reynolds number of 1, 00,000 based on the leading edge diameter. The test model wall temperature is measured using non-contact type infra-red camera after the steady state main stream and coolant flows have been achieved. The film effectiveness measurements are made with the mainstream at ambient temperature, coolant temperature and with the wall temperature measured as adiabatic wall temperature, as the surface is unheated and well insulated. The local wall temperature is mixture temperature of the coolant and mainstream. Thus, the film effectiveness is found using the following relation.

$$= \frac{(T_m - T_w)}{(T_m - T_{c)}} \qquad (1)$$

The blowing ratio (BR) is maintained using the ratio of coolant to mainstream mass flux ratio, the relation is given by

$$B.R = \frac{(\rho c * Vc)}{(\rho m * Vm)} \qquad (2)$$

The main stream flux ($\rho_\infty V_\infty$) was estimated from the measured mainstream velocity and the estimated mainstream density based on the static pressure and total temperature measured in the test section. The coolant mass flux ($\rho_c V_{c)}$ was estimated by dividing the measured mass flow by the total cooling hole area based on the inlet diameter of the film cooling hole. After establishing the required blowing ratio, the coolant temperatures and the model surface temperatures measured by the thermocouples were continuously monitored to have the required density ratio.

An uncertainty analysis performed indicates that the uncertainty in the calculated blowing ratio was $\pm$ 0.06 based on mainstream velocity uncertainty of $\pm$0.05 m/s and coolant velocity uncertainty of $\pm$0.6m/s. The IR thermogram test model wall temperature uncertainty is in the order of $\pm 2^0$C.

D. Heat transfer Coefficient Measurements

The heat transfer coefficients are measured with mainstream and coolant air at the ambient temperature with the test surface at heated constant heat flux condition. The test model made of low conducting material to avoid heat losses from the noncontact side of the model. The test surface is wound with the 0.15mm thin s.s sheet and is connected in series to the electrical power through brass bus bars. The test model surface, supplied with electrical power and heated, serves as a constant heat flux surface during the heat transfer experiments. The calibrated thermocouples soldered underside of the s.s sheet acts as a reference for correcting the thermogram data. The test surface is exposed to the required main stream and coolant flows. The electrical power is supplied to the s.s sheet at a high current and low voltage through step down transformer and dimmer stat. After achieving a steady state, the test wall temperature data is captured to find the local heat transfer coefficient values. Circuit current and voltage will provide the total heat input to the test surface i.e.

The total heat input to the surface is calculated by measuring current and voltage input to the surface.

Where Q = Heat Input in Watt
V = Voltage in Volts
I = Current in ampere

$$Q = V \times I$$

Heat transfer coefficients can be calculated as

$$h = \frac{q}{(T_w - T_m)} = \frac{q_{gen} - q_{loss}}{(T_w - T_{aw})}$$

The conduction loss data of non contact side is found separately for both the considered models, which is accounted for the heat transfer coefficient calculations. For the generation of conduction loss, the leading edge models are insulated with glass wool material to avoid the heat loss from the model. Experiments are carried out by supplying the electric current to test model through a brass bus bars attached

to the S.S sheet wound on the leading edge model. From the test it is found that when the voltage increases the heat loss in plate also increases for the considered two models. And this linear conduction loss is accounted in the heat transfer coefficient distribution calculations.

Voltage Vs Current experiments are carried out for both models. Electric wires are soldered between holes at the known distances. The test surface current is increased by supplying voltage, the linear equation is found to calculate the current from the applied voltage. The product of voltage and current is used to find the gross heat input to the test surface during the heat transfer coefficient experiments.

III. Computational Details of Present Study

Film cooling effectiveness and heat transfer coefficient data is calculated experimentally for different B.R of 1.0, 1.50, 2.0 and 2.50 for the compound angled blade leading edge with different hole diameter models. The same has been tried with film cooling effectiveness numerically using ICEM CFD meshing and ANSYS Fluent and CFD Post is used for this study to have the comparison with the experimental data.

A. Geomentry of Computational Model

In the computational analysis, the same gas turbine blade leading edge model is used, generated for experimental models using the solid works. The computational model consists of leading edge of gas turbine blade with the flow duct. Computational model size of 320 x 210 x 384 mm with leading edge outer diameter of 89mm and inner diameter of 65mm, with the five rows of film cooling holes, each row having five holes of 4mm diameter with the hole pitch of 21mm. The second computational model is also generated with the same geometrical parameters at 5.6mm film hole diameter. The generated computational model size is same for both the models. Computational model is prepared as per experimental test section and only half of length of the test section is taken and symmetry portion of the leading edge is taken to avoid more number of element cells and analysis running time.

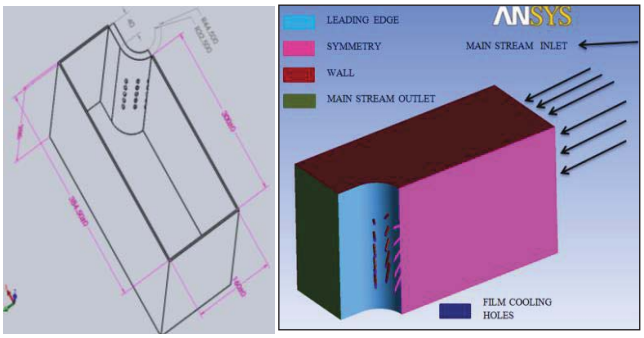

Fig. 8. The Geomentry of Computational Domain.

Computational model is prepared using solid works and imported in Ansys ICEM CFD for meshing purpose; the geometry of computational domain is shown in the Fig. 8.

The mesh is generated for the considered geometry of the domain. The preprocessor, solver and Postprocessor modules employed by ANSYS 14 Fluent are used in this computational analysis. For the assumed y^+ value of 30 near wall adjacent for the turbulence model the obtained δy=0.158. The different meshes have been generated and the grid dependency is plotted for all these considered mesh sizes and is as shown in Fig. 9. For the considered element numbers, the mesh with 661084 elements and higher showed same results. Hence the lowest mesh size of 661084 elements is considered as suitable mesh for computational analysis.

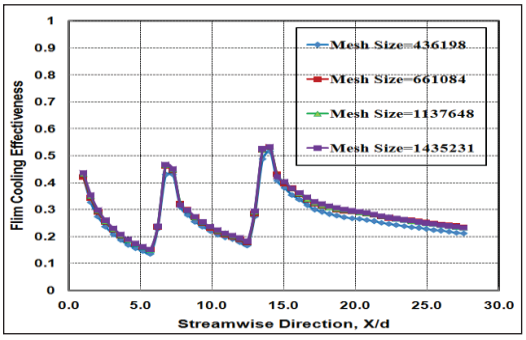

Fig. 9. Grid dependency for the film cooling effectiveness

B. Boundary Conditions

TABLE II. Boundary Conditions

SI. No.	PART	BOUNDARY TYPE
1	Leading Edge	Wall
2	Coolant Inlet and Main Stream Inlet	Pressure Inlet
3	Main Stream Outlet	Pressure Outlet
4	Symmetry	Symmetry
5	Wall	Wall

In the process of finding the solution for film cooling effectiveness the k-omega SST, k-epsilon standard and k-epsilon realizable turbulence models are tried to get the solution for this model, among which the k-epsilon realizable turbulence model gives the better solution, which is nearer to the experimental values as shown in Fig. 10.

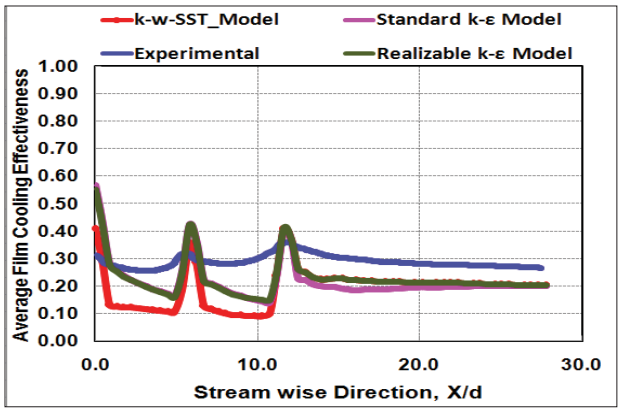

Fig. 10. Average film cooling effectiveness for the Different Turbulance models avaliable in Fluent Solver.

Hence, the k-epsilon realizable turbulence model is used in solver for all the blowing ratios for the CFD

simulation. The type of boundary conditions applied in the computational model are shown in Table II. The boundary condition values are used same as that of experimental test conditions and the adiabatic condition is ensured by considering the boundary conditions as a leading edge wall with a zero heat flux condition.

IV. Results and Discussion

The mass flow measurements are done by supplying the secondary air to the model through the coolant chamber by varying the coolant chamber pressure and the coefficient of discharge for the model 1 with 4mm hole diameter is found as 0.82 and for the model 2 with 5.6mm hole diameter is found as 0.74.

A. Adiabatic Film Cooling Effectiveness Measurements

Adiabatic film effectiveness is calculated experimentally and numerically using CFD for two leading edge gas turbine models with different hole diameters i.e. model 1 with 4mm hole diameter and model 2 with 5.6 mm hole diameter with same compound angles and pitch of 21 mm. The Infra red temperature contours are used to calculate the cooling effectiveness during the experiments. And in a similar manner the cooling effectiveness is also extracted numerically using temperature contours at the similar test conditions along streamwise direction and these results are compared.

1) Experimental and Numerical Results For Compound angled Model 1 with the hole diameter of 4mm

The experimental and CFD temperature contours for the model 1 at the blowing ratios of 1.0, 1.50, 2.0 and 2.50 respectively are shown the figures from Fig. 11 to Fig. 14.

From both the experiments and CFD it is found that, at the B.R of 1.0 coolant films were not found near stagnation line due to low pressure which can be visualized from the Fig. 11. Further with the increase in B.R the coolant film was found over the hole region and downstream of holes. Fig. 11 to 14 shows the flow pattern contours of film cooling effect obtained from experimental and numerical simulation at different blowing ratios. The similar trends are observed in both the experimental and CFD Contours.

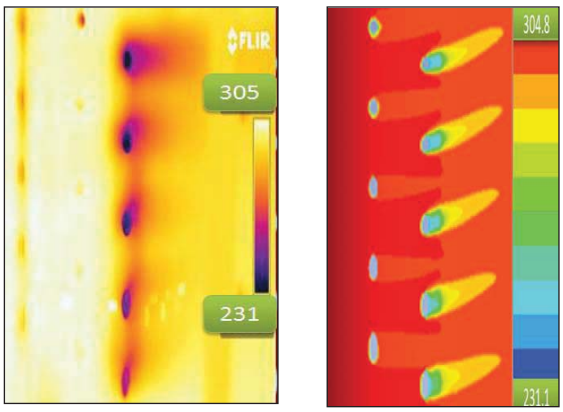

Fig. 11. M1_ Experimental and CFD Contours at BR=1.0

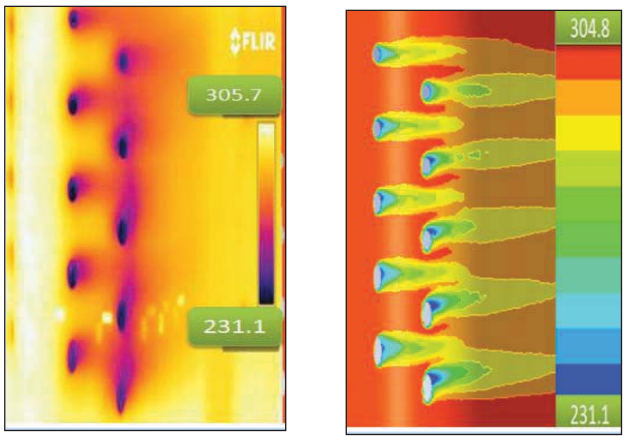

Fig. 12. M1_Experimental and CFD Contours at BR=1.50

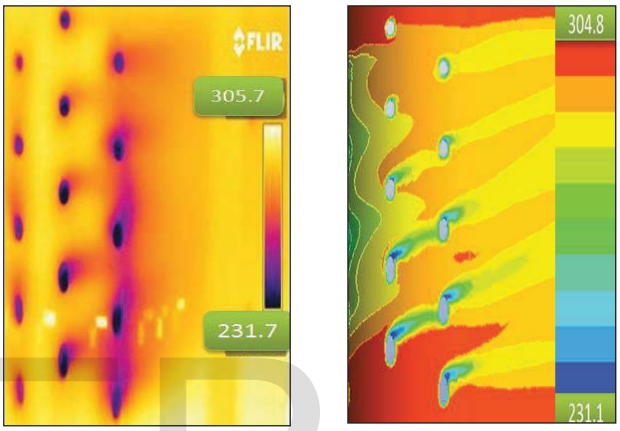

Fig. 13. M1_Experimental and CFD Contours at BR=2.0

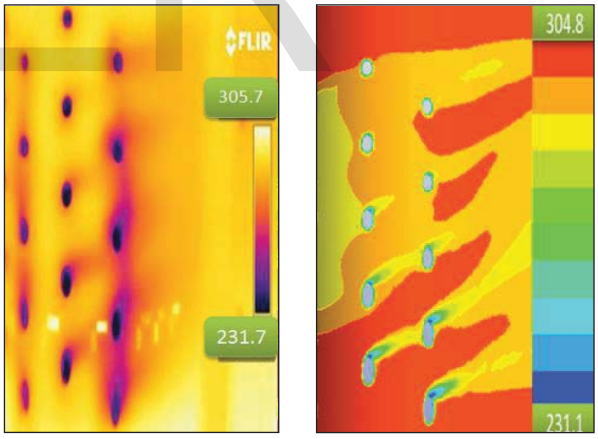

Fig. 14. M1_Experimental and CFD Contours at BR=2.50

The experimentally found averaged film cooling effectiveness plots in stream wise direction for all the four considered blowing ratios are shown in Fig. 15. Similarly, Fig. 16 shows the film cooling effectiveness plots found by CFD simulation along stream wise direction.

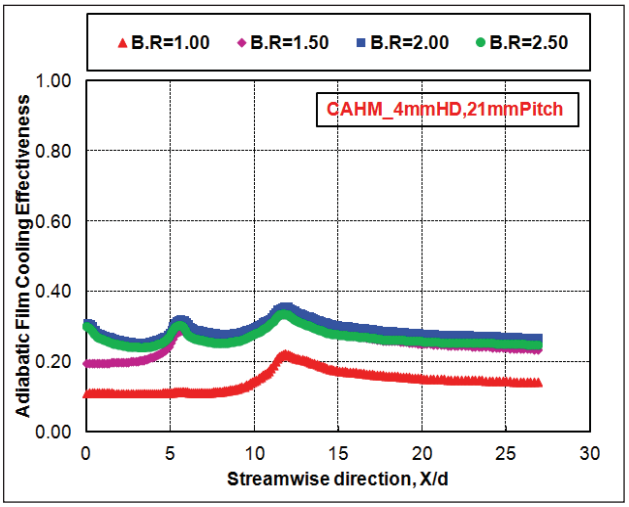

Fig. 15. M1_ Experimentally Averaged Film Cooling Effectiveness Plots in Streamwise Direction at different BR.

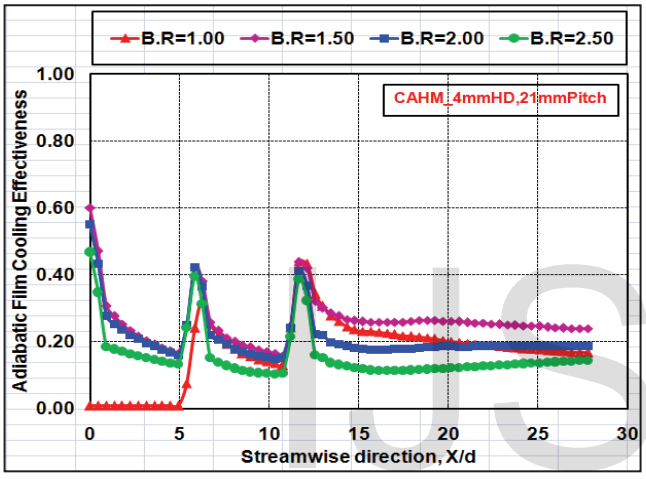

Fig. 16. M1_Numerically (CFD) Averaged Film Cooling Effectiveness Plots in Streamwise Direction at All BR

From the Figs. 11 to 16, it is observed that film cooling effectiveness is increases with increase in B.R upto a certain value of B.R. The experimental analysis shown the higher cooling effectiveness at B.R 2.0, where as the numerical results has shown the higher cooling effectiveness at B.R 1.50. CFD has shown the similar trends of film cooling effectiveness values as that of experimental results. Both the experimental and CFD has shown the decrease in film cooling effectiveness above B.R of 2.0. Hence, blowing ratio of 2.0 can be considered as optimised B.R for this configuration. The peaks in the results indicate the location of film cooling hole rows along stream wise direction.

2) Experimental and Numerical Results For Compound angled Model 2 with hole diameter of 5.6mm.

The experimental and CFD temperature contours for the model 2 at the blowing ratios of 1.0, 1.50, 2.0 and 2.50 respectively are shown in the figures from Fig. 17 to 20.

From both the experiments and CFD it is found that at B.R of 1.0 coolant films were not found near stagnation region due to low pressure, which can be visualized from the Fig. 17. Further with the increase in B.R, the coolant film was found near stagnation region too and downstream of holes. Fig. 17 to 20 shows the flow pattern contours obtained from experimental and numerical Simulation. The similar trends are observed in both the experimental and CFD Contours.

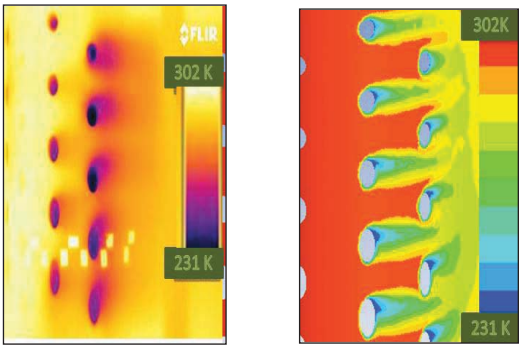

Fig. 17. M2_Experimental and CFD Contours at BR=1.0

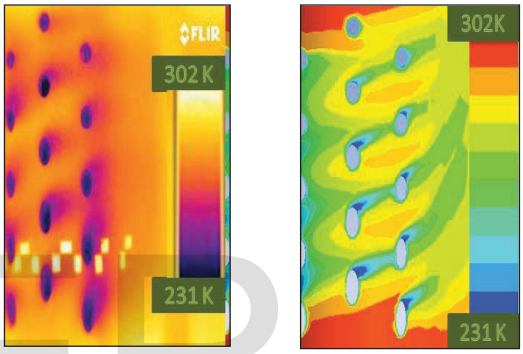

Fig. 18. M2_Experimental and CFD Contours at BR=1.50

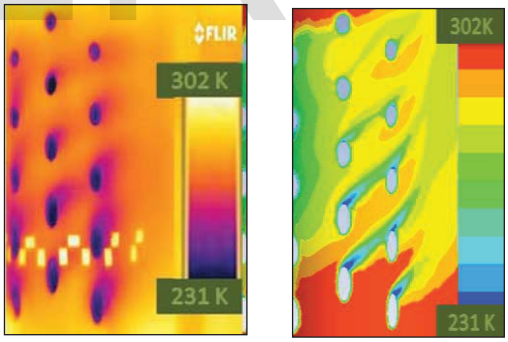

Fig. 19. M2_Expperimental and CFD Contours at BR=2.0

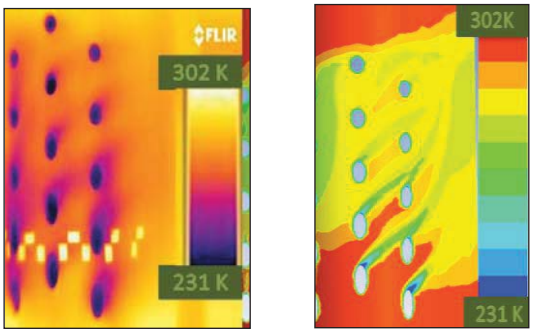

Fig. 20. M2_Expperimental and CFD Contours at BR=2.50.

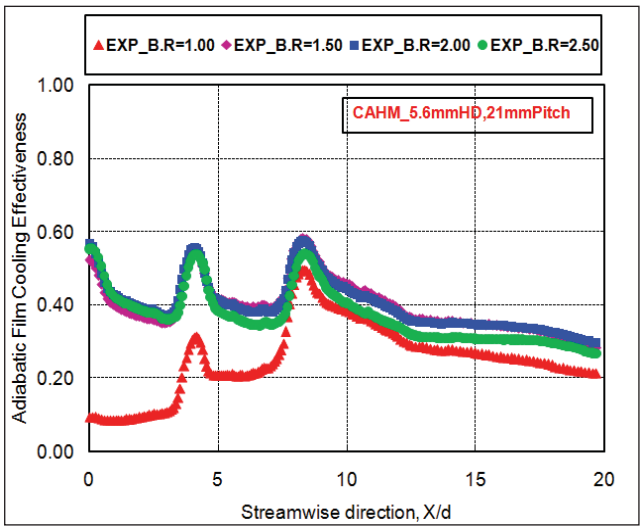

Fig. 21. M2_ Experimentally Averaged Film Cooling Effectiveness Plots in Streamwise Direction for All Blowing Ratios.

The experimental average film cooling effectiveness plots in stream wise direction for all the four considered blowing ratios are shown in Fig. 21. Similarly, Fig. 22 shows the film cooling effectiveness plots found by CFD simulation.

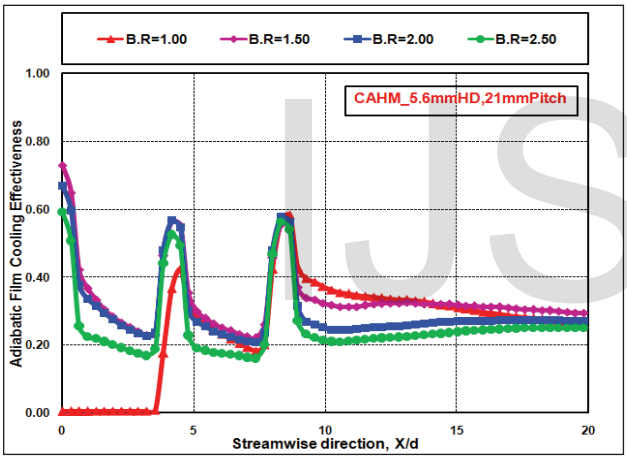

Fig. 22. M2_Numerically Averaged Film Cooling Effectiveness Plots in Streamwise Direction for All Blowing Ratios.

From the Figs. 17 to Fig. 22, it is observed that film cooling effectiveness has increased with increase in B.R upto 1.50. Further increase in B.R has not shown considerable increase in film cooling effectiveness. The same is observed in both the experimental and CFD results. Hence the blowing ratio of 1.50 can be considered as optimised B.R for this configuration. The peaks in the results indicate the location of film cooling hole rows along stream wise direction.

B. Comparison of film cooling effeectiveness, Model 1 and Model 2

The Fig. 23 shows the comparision of experimentally averaged film cooling effectivenesss for model 1 and model 2 at BR 1.50. Similarly the Fig. 24 shows the comparision of numerically averaged film cooling effectivenesss for model 1 and model 2 at BR 1.50.

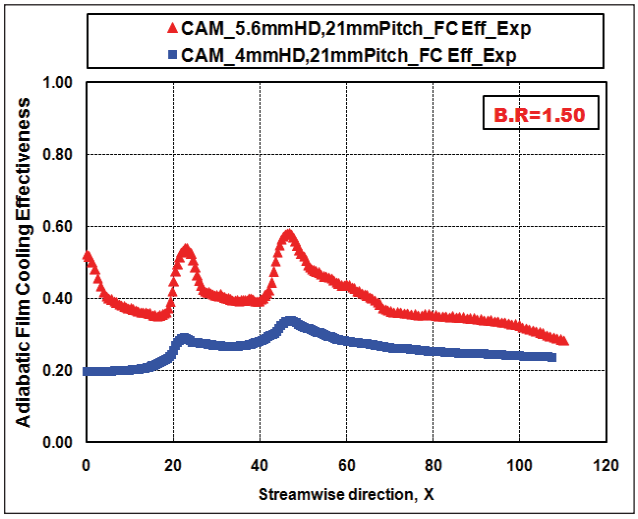

Fig. 23. M1 and M2_Comparision of Experimentally averaged film cooling effectivenesss at BR 1.50.

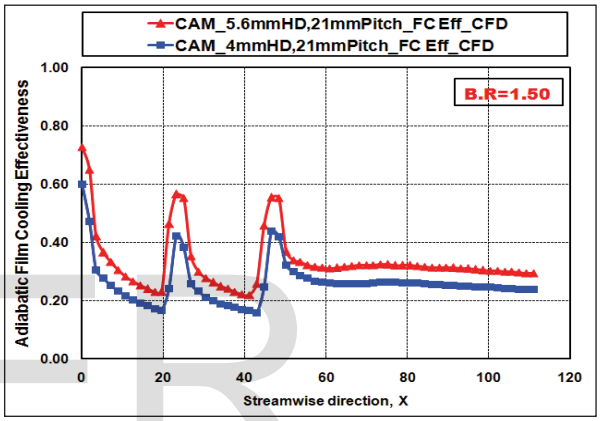

Fig. 24. M1 and M2_Comparision of CFD_Numerically averaged film cooling effectivenesss at BR 1.50

From Figs. 23 and 24, the model 2 with hole diameter of 5.6mm shows higher cooling effectiveness compared to model 1 having 4mm hole diameter. The same effect is observed by both the experimental and numerical results.

C. Heat transfer coeficients Measurements

Heat transfer coefficient distribution is calculated both experimentally and numerically for two leading edge gas turbine models i.e. M1 and M2. During the CFD prediction of heat transfer coefficient experiments the heat flux is given on the leading wall in order to heat the wall surface. The results are extracted similar to film cooling effectiveness measurements for different blowing ratios.

Experimentally and numerically evaluated temperature contours are taken and the average heat transfer coefficients at different blowing ratios along the stream wise directions are found. These results are as shown in below figures for the model 1.

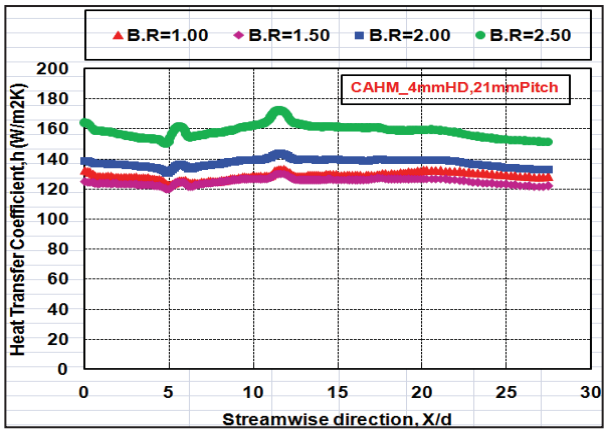

Fig. 25. M1_Experimentally averaged heat transfer coefficients at all BR.

Figs. 25 and 26 shows the experimental and numerical results of heat transfer coefficient for considered blowing ratios. The heat transfer coefficient found increases with increase in blowing ratio along the stream wise direction. The same has been observed from both the experimental and CFD results. The peaks in the results indicate the location of film cooling hole rows along stream wise direction.

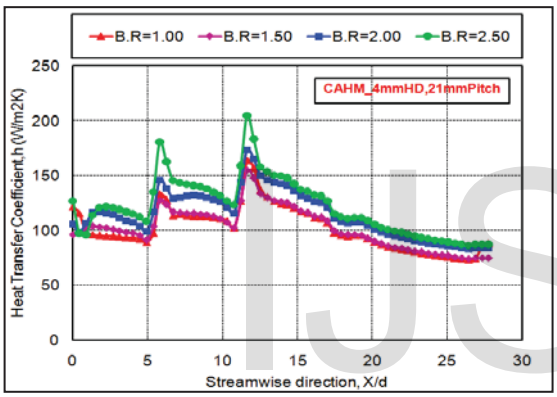

Fig. 26. M1_Numerically (CFD)averaged heat transfer coefficients at all BR.

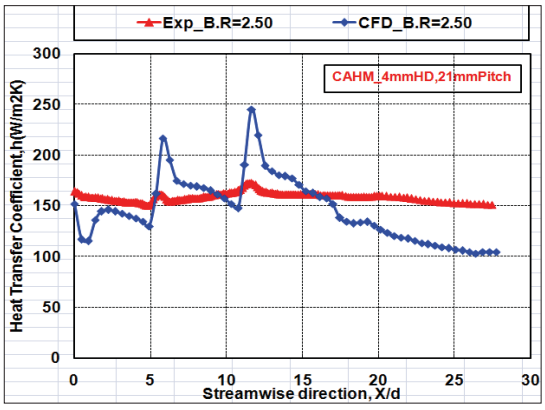

Fig. 27. M1_Experimental and CFD comparision of averaged heat transfer coefficients at a BR 2.50

Fig. 27 shows the comparative plot of experimental and numerical results of heat transfer coefficient at blowing ratio 2.50 along the stream wise direction for the model 1. Both the experimental and CFD shows the similar results upto the x/d of 18 along the streamwise direction. The shift in the down stream region is due to the more heat levels in the experimental case with bus bars at the end, where as in CFD a constant heat flux is imposed on the leading edge test surface.

Fig. 28 shows the experimentally found heat transfer coefficient values of model 2 at the considered blowing ratios. The peaks in the results indicate the location of film cooling hole rows along stream wise direction. The heat transfer coefficient values found increasing with the increasing blowing ratio.

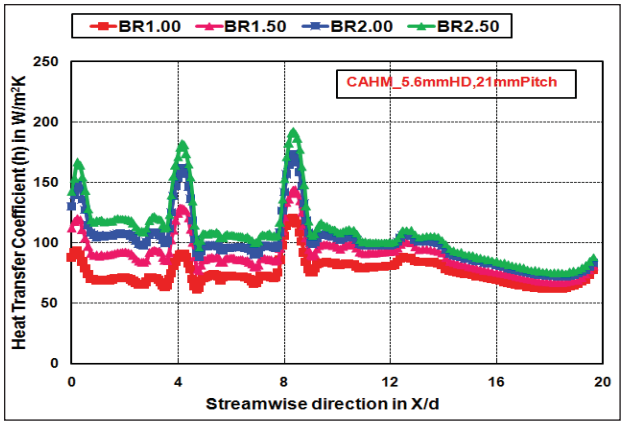

Fig. 28. M2_Experimentally averaged heat transfer coefficients at all BR

V. Conclusions

Film cooling is one of the best cooling technologies for external cooling of gas turbine leading edge. This study investigates film effectiveness and heat transfer coefficients distribution both experimentally and numerically. Experiments were conducted at CSIR-NAL Film cooling test facility with constant mainstream Reynolds number of 100000 and varying the blowing ratio from 1.0, 1.5, 2.0 and 2.5 at a density ratio of 1.30 for film cooling effectiveness and density ratio of 1.0 for heat transfer coefficient experiments. Numerical investigations were conducted with help of ANSYS 14, ICEM CFD Meshing and FLUENT V6.

From numerically calculated adiabatic film cooling effectiveness, initially the three turbulence models i.e. k-ω sst, k-ε standard and k-ε realizable turbulence models are tried to get the solution with compound angled model, among which the k-ε realizable turbulence model shows the results nearer to the experimental values. Hence, the k-ε realizable turbulence model is used for the CFD simulation.

From both the experimental evaluation and CFD estimation, for the Model 1 Film cooling effectiveness is found increasing with the increase in B.R from 1.0 to 2.0 and further increase in B.R did not shown any considerable improvement and thus the optimized blowing ratio for the model 1 can be considered as 2.0. Model 2 shows the increase in film cooling effectiveness with the increasing B.R up to 1.50 and it is observed the higher value of film cooling effectiveness from temperature contours and graphs at the B.R of 1.50 and further increase in the blowing ratio above 1.50 there is no increase in film cooling effectiveness for this model. Hence, the optimized blowing ratio for the model 2 can be considered as 1.50. The heat transfer coefficients found to be increasing with the increase in B.R among the considered range on both the models.

The model 2 with hole diameter of 5.6mm shows higher cooling effectiveness compared to model 1 having 4mm hole diameter. The same effect is observed from both the experimental and numerical results. Hence we can conclude that the higher film hole diameter at the same pitch and flow conditions provides the higher cooling effectiveness. This is due to the more flow coverage and conduction effects.

From CFD, the adiabatic film cooling effectiveness and heat transfer values have shown similar values compared to the experimental values. Here we calculated the laterally averaged adiabatic film cooling effectiveness and laterally averaged heat transfer coefficients along the streamwise direction and for the entire blowing ratios of 1.0 to 2.50. In all the result plots it is observed that the peaks values clearly indicate that adiabatic film cooling effectiveness values near the holes. And the CFD contours also shown the meaningful similar results as that of the experimental contours with same flow patterns, as observed from temperature contours obtained from infrared camera and CFD at all blowing ratios.

Acknowledgment

The authors wish to thank Mr. Manjunath P., Head, Propulsion Division and Director, NAL, Bangalore for permitting this work to be done at NAL. The authors also would like to thank Mr. Maria Arockiam, Mr. Sanmuganantham and Mr. Ravishankar N for their help in fabrication, assembling and assisting to conduct experiments and for their suggestions during this course of work. Authors would like to thank all the others who have directly or indirectly helped us in carrying out this work.

Nomenclature

BR	-	Blowing Ratio
DR	-	Density Ratio
AR	-	Area Ratio
ρc	-	Coolant Density (kg/m^3)
ρm	-	Mainstream Density (kg/m^3)
h	=	Heat Transfer Coefficients in w/m^{2}k
q	=	Net Local Convective Heat Flux the Foil Surface in w/m^2
q_{gen}	=	Surface Generated Heat Flux from Voltage-Current Measurement in w/m^2
q_{loss}	=	Local Heat Loss and Is a Function of the Local Wall Temperature w/m^2
T_w	=	is the Local Steady State Foil Temperature (Local Wall Temperature) in k
T_{aw}	=	is the Local Adiabatic Wall Temperature in k.
T_m	=	Mainstream Temperature in k.
I	-	Current Supplied
W	-	Width of stainless steel sheet (mm)
P_c	-	Inlet Pressure (kPa)
P_t	-	Outlet Pressure (kPa)
Vc	-	Coolant Velocity (m/s)
V_m	-	Mainstream Velocity (m/s)
	-	Film cooling effectiveness
E	-	Voltage drop

References

[1] JE-Chin Han, Sandip Dutta et.al , "Gas Turbine Heat transfer and cooling technology," "Scond Edition", ISBN-13:978-1-4398-5568-3, pp. 21-40.

[2] JE-Chin Han and Srinath Ekkad, "Recent Development In Turbine Blade Film Cooling," International Journal of Rotating Machinery, Vol 7, No 1, 2001, pp. 21-40.

[3] James E. Mayhew, James W. Baughn, Aaron R. Byerley, "The Effect of Freestream Turbulence on Film Cooling Adiabatic Effectiveness", *International Journal of Heat And Fluid Flow*, Vol. 24, 2003, pp.669-679.

[4] LI Shaohua Tao Peng, Li- Xian Liu, Ting-ting GUO , Bin Yuan, "Numerical Simulation of Turbine Blade Film cooling with Different Blowing Ratio and Hole to hole space", *International Conference on Power Engineering*, 2007, pp 1372-1375.

[5] Ali Rozati, Danesh K. Tafti "Effect of Coolant -Mainstream Blowing Ratio on Leading Edge Film Cooling Flow and Heat Transfer-Les Investigation" ,*International Journal of Heat and Fluid Flow*, Vol. 29, 2008, pp. 857-873.

[6] Cruse, M.W., Yuki U. and Bogard D.G. "Investigation of various parametric influences on leading edge film cooling" *ASME Paper 97-GT*-296.